RSC Advances

ROYAL SOCIETY OF CHEMISTRY

www.rsc.org/advances

Journal Name

ARTICLE

An Electrochemical Study Based on Thymine-Hg-Thymine DNA Base Pairs Mediated Charge Transfer Process

Received 00th January 20xx,

Accepted 00th January 20xx

DOI: 10.1039/x0xx00000x

www.rsc.org/

Ensheng Xu[1], Yanqin Lv[1], Jifeng Liu[1, 2]*, Xiaohong Gu[3], Shuqiu Zhang[3*]

Onto Au surface adsorbed DNA monolayer composed of double stranded of 25 base pairs, and at the gold surface and distal part were matched base pairs, while at the middle of DNA monolayer were $(TT)_n$ mismatched pairs. Methylene blue was attached at the end DNA monolayer via a C_6 alkyene linker and acted as the electrochemical probe. Upon addition of mercury ions (Hg(II)), thymine-Hg-thymine ($(T\text{-}Hg(II)\text{-}T)_n$) was formed through metal coordination between DNA duplexes. The charge transfer (CT) properties of the DNA monolayer was studied using Laviron's theory and it was found that when $n \leq 6$, the kinetics of CT followed the order: matched DNA base pairs < DNA duplexes with $(TT)_n$ < DNA duplexes with $(T\text{-}Hg(II)\text{-}T)_n$ and the CT kinetics increased with increasing n. The conformation of DNA monolayer adsorbed onto Au (111) was investigated using atomic force microscopy (AFM) and it was found that duplexes structure was remained when $n \leq 6$. The formation of $(T\text{-}Hg(II)\text{-}T)_n$ brought a more smooth DNA monolayer surface than that composed of match DNA base pairs. However, an interesting phenomenon was found when $n \geq 12$, that is $(T\text{-}Hg(II)\text{-}T)_n$ conformation was formed between different DNA strands and the this inter-DNA $(T\text{-}Hg(II)\text{-}T)_n$ structure caused DNA monolayer deformed and CT not occur along the DNA base pairs.

Introduction

The molecular π-stack of base pairs within double-strand DNA (dsDNA) has been shown to mediate charge transfer (CT) reactions, which has received a substantial attention because of its biological significance in DNA damage and DNA repair mechanisms as well as the DNA electronic devices.[1] Because this CT property of DNA depends on coupling within the base pair stacking, DNA CT is sensitive to static and dynamic perturbations in base pair structures.[2] Several techniques or types of assemblies have been employed for studying DNA-mediated CT: [3] a) electrochemical method, where molecular self-assembly of dsDNA on electrode was used to mediate electron transfer between the electrode and the redox active intercalator bound to the DNA at a site remote from the electrode surface;[4-6] b) DNA-mediated CT (hole) between photoexcited fluorophor and quencher;[7,8] c) DNA-mediated CT (oxidative radicals) between photoexcited oxidizer and oxidizable groups (DNA bases, e.g. guanine). [9,10]

[1]Department of Chemistry, Liaocheng University, Liaocheng, 252059, Shandong, China.
[2]*Key Laboratory of Food Nutrition and Safety, Ministry of Education of China, Tianjin University of Science and Technology, Tianjin 300457, China.*
Email: liujifeng111@gmail.com; tel & fax, 022-60602795
[3]*Shandong Provincial Key Lab of Test Technology on Food Quality and Safety, Shandong Academy of Agricultural Sciences, Jinan 250100, China.*
Email: zxszsq@163.com

Comparatively, electrochemical detection of base pair stacking perturbations may lead to diagnostic applications of DNA CT due to the simplicity of electrochemical methods.[2] Usually, electrochemical reduction of the distantly bound intercalator was conducted to study the CT through the base pair stacking under a negative potential. Perturbation in base pair stacking would cause a significant loss in CT efficiency and the sensitivity to base pair stacking provides the foundation for applications of DNA CT to probe DNA structure.[11] So DNA mediated CT process have been applied to sensing DNA structures, such as base mismatch in fully hybridized DNA duplexes,[12] conformation of DNA (A-, B-, and Z-Form DNA), [11] base lesions, [13] binding of proteins[14] or cisplatin to DNA.[15]
This DNA structure-depending CT electrochemical sensitivity may find application in biological processes, [16] such as repair of photo-induced DNA lesions by CT process, localization of oxidative lesion and the corresponding mechanisms for antioxidant protection.[16] In the later case, it is well known that oxidative lesions of DNA by reactive oxygen species (ROS) are the most widespread damage in living organisms. Hydroxyl radicals (•OH), singlet oxygen, superoxide anion are main ingenuous ROS inducing DNA oxidation damage.[17-19] Based on this mechanism, we developed a TiO_2@γ-Fe_2O_3/$(AT)_n$/dsDNA/Au composite monolayer assembly to read the diffusion distance of •OH.[20]
A lot of works have been reported on DNA base pairing via metal coordination acting as the driving force and as an

alternative to hydrogen bonding.[21] The metal coordination is an stronger bonding and DNA duplexes possessing such metallo-base pairs usually exhibited higher thermal stability than natural hydrogen-bonded DNAs. Such kind of metal-responsive functional DNA molecules may find use in DNAzymes and DNA machines.[21] It is well-known that in the presence of Hg(II) ions, thymine-thymine (TT) mismatch pair would form neutral metallo-base pair (T-Hg(II)-T) as originally proposed previously. [22,23] An this T-Hg(II)-T complexes have higher thermal stability than matching DNA base pairs, such as A–T.[23] The T-Hg(II)-T chemistry was of significance in probing defects in DNA or the assay of Hg(II) in the environment. However, the study of the effect of metal-mediated DNA base pairing on the CT process of DNA is rarely reported. The conductance measurement of the DNA duplexes containing one H-Cu(II)-H base pair has been reported to be comparable to that of natural DNA duplexes, indicating that the H-Cu(II)-H base pair favors CT similarly to natural DNA matching base pairs.[24] Theoretical and fluorescence studies found that for DNA duplex containing T-Hg(II)-T, the overlap of the bases was favorable for CT at low temperatures. CT was driven by Hg changing the spatial overlap of bases.[25] At higher temperature, CT efficiency increased due to the thermal motions for all DNA duplexes, and the matching DNA had the highest CT efficiency. [25] Despite these efforts being devoted to the CT of metal-mediated DNA base pairing, there are still fundamental issues that have not been explained.

Here, based on DNA mediated electrochemical process, the CT kinetics were compared in standard dsDNA, dsDNA with mismatched T-T base pairs, and dsDNA with a T-Hg(II)-T base pairs. Double strands of 25 base pairs was adsorbed onto the gold surface to form a monolayer, while at the middle of DNA monolayer was $(TT)_n$ mismatch pairs. In the presence of Hg(II) ions, T-Hg(II)-T was formed in the DNA duplexes. At modified electrode surface, methylene blue (MB) was attached at the end of dsDNA strand. Under a negative potential, from the electrochemical reduction currents of MB, we can determine CT properties of DNA duplexes.

Gelelectrophoresis

Figure 1 is the gel electrophoresis analysis of the above samples. From the gel electrophoresis image of fluorescence signal it is showed that matched DNA, dsDNA with $(TT)_1$, dsDNA with $(TT)_3$, dsDNA with $(TT)_6$ can be hybridized to form duplexes. Comparatively, the dsDNA with $(TT)_{12}$ sequence was less stable than the other dsDNA, indicating the DNA sequence with $(TT)_{12}$ can not be able to hybridize.

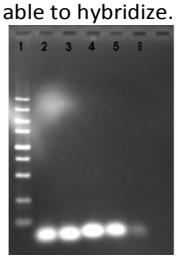

Figure 1. Gel electrophoresis image for assay of the DNA duplexes. Lanes 1 and 6: mark, matched DNA, dsDNA with $(TT)_1$, dsDNA with $(TT)_3$, dsDNA with $(TT)_6$, dsDNA with $(TT)_{12}$, respectively.

Surface density and coverage of adsorbed DNA monolayer

The cationic redox molecules, $Ru(NH_3)_6^{3+}$ were electrostatically associated with the anionic DNA backbone and provide charge compensation to the backbone at a low ionic strength electrolyte. The surface density of DNA probes on the surface was calculated from the number of cationic redox ($Ru(NH_3)_6^{3+}$) and determined by applying integrated Cottrell equation,[26]

$$Q = \frac{2nFAD_0^{1/2}C_0^*}{\pi^{1/2}} t^{1/2} + Q_{dl} + nFA\Gamma_0 \qquad (1)$$

where n is the number of electrons per molecule for reduction, F is the Faraday constant (C/equiv), A is the electrode area (cm^2), D_0 is the diffusion coefficient (cm^2/s), C_0* is the bulk concentration (mol/cm^2), Q_{dl} is the capacitive charge (C), and is $nF\Gamma_0$ the charge from the reduction of Γ_0 (mol/cm^2) of the adsorbed $Ru(NH_3)_6^{3+}$. The term Γ_0 designates the surface excess and represents the amount of $Ru(NH_3)_6^{3+}$ confined near the electrode surface. The chronocoulometric intercept at t = 0 is then the sum of the double layer charging and the surface excess terms. The surface excess is determined from the difference in chronocoulometric intercepts for the identical potential step experiment in the presence and absence of $Ru(NH_3)_6^{3+}$(Figure 2).

The DNA probe was adsorded on Au (111) facet of Au electrode surface via Au-S complex. In presence of $Hg(II)^{2+}$ ions, if the thiol group of DNA probe react with the $Hg(II)^{2+}$ ions, the DNA will be removed from the Au surface and result in a lower surface density. It was found that the surface density of well matched DNA monolayer measured was about 1×10^{13} molecules/cm^2 and did not change obviously after the DNA modified electrode was immersed in 10 nM $HgCl_2$ solution for 30 min. The self-assembled DNA monolayer on Au surface used in this work was stable in presence of Hg(II) ions. Taking the diameter of DNA helix as 2 nm, the surface coverage of DNA monolayer at the Au surface was about 40%, showing a highly packed monolayer.

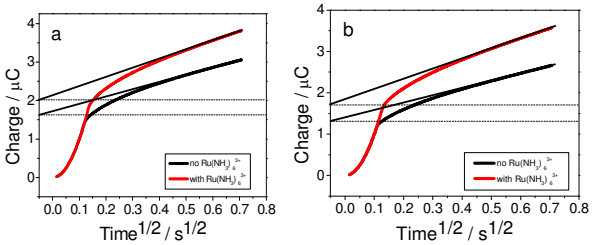

Figure 2.Chronocoulometric response curves for the probe dsDNA modified electrode in 10 mM Tris buffer (pH 7.4) in the presence and absence of 50 μM $Ru(NH_3)_6^{3+}$(a) and interact with Hg(II) (b).

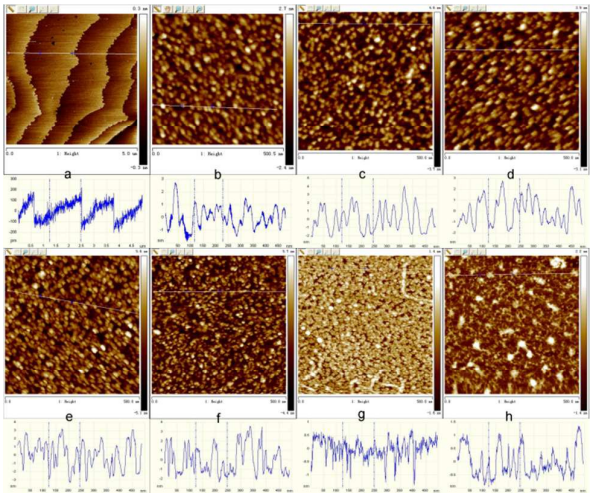

Figure 3. AFM image of DNA monolayer on Au(111). (a) fresh Au(111)，(b) matched dsDNA, (c) dsDNA with $(TT)_3$, (d) dsDNA with (T-Hg(II)-T)$_3$, (e) dsDNA with $(TT)_6$, (f) dsDNA with (T-Hg(II)-T)$_6$, (g) dsDNA with $(TT)_{12}$, (h) dsDNA with (T-Hg(II)-T)$_{12}$.

AFM imaging

From the AFM image of Au(111), it was shown that an atomically flat multi-stage facets and the roughness of the facet is 0.15 nm (Figure 3a). DNA monolayers were examined to visualize the DNA surface coverage and distribution of individual helices within the monolayer. A typical AFM image of the matched dsDNA monolayer is shown in Figure 3b and revealing no large-domain clustering (packed into cluster). Notably, the images show some monolayer stratification, consistent with compact film structure and small clusters of DNA that are remarkably uniform in size (20 nm) and shape. The number of DNA helices contained in a microcluster is approximately 6.25×10^{12} molecules/cm^2, which is consistent with that obtained form chronocoulometry.

DNA monolayer with $(TT)_3$ (Figure 3c) and $(TT)_6$ (Figure 3e) mismatches showed also uniform surface coverage and distribution of micro domains. For $(TT)_3$ duplexes, after treated with Hg(II) ions (Figure 3d), the height of DNA duplexes increased slightly observed from the height distribution, indicating the existence of T-Hg(II)-T complex in DNA duplexes increased the rigidity and became stiffer. However, for DNA duplexes with $(TT)_6$ mismatches, after formation of T-Hg(II)-T complex (Figure 3f), the height of DNA monolayer decreased and maybe DNA duplexes bent after formation of (T-Hg(II)-T)$_6$ complex. That means that (T-Hg(II)-T)$_6$ structure may adopt a less rigid straight conformation, but the SAM still showed a compact monolayer coverage distribution.

DNA monolayer with $(TT)_{12}$ mismatches (Figure 3g) showed quite different morphology form matched DNA SAM and those monolayers containing $(TT)_3$ or $(TT)_6$ mismatches. DNA molecules containing $(TT)_{12}$ easily tilted or even lie upon the Au(111), thus leading to measured height values compatible with the axial width of the molecule instead of its end-to-end length, but still showed a compact coverage. DNA molecules containing $(TT)_{12}$ may not be able to hybridize well and the sequence $(TT)_{12}$ might split causing DNA molecules lie down. Upon addition of Hg(II) ions (Figure 3h), DNA molecules lying upon the Au(111) shrinked and gave a appearance of aggregated DNA wire at Au(111). The height of DNA wire was about that of axial width. And the substrate of Au(111) was exposed indicating that T-Hg(II)-T complex may form between different DNA molecules and cause the aggregation to form larger DNA cluster(Scheme 1). In this case, DNA molecules containing $(TT)_{12}$ and (T-Hg(II)-T)$_{12}$ was not suitable for DNA duplex mediated electrochemical CT study.

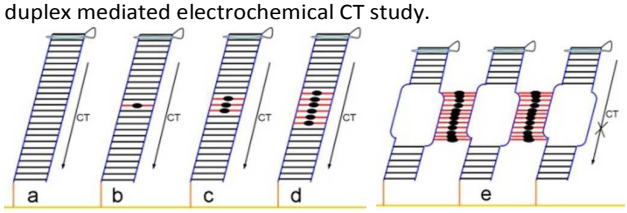

Scheme 1. CT process of dsDNA with (T-Hg(II)-T) sequench. (a) matched dsDNA, (b) dsDNA with (T-Hg(II)-T)$_1$, (c) dsDNA with (T-Hg(II)-T)$_3$, (d) dsDNA with (T-Hg(II)-T)$_6$, (d) dsDNA with (T-Hg(II)-T)$_{12}$.
(T-Hg(II)-T) ; matched DNA bases; C_6 linker; methylene blue.

The Electron-Transfer Rate of the DNA Self -assembled Monolayers

The CT rates were determined by applying Laviron analysis to CV (Figure 4,5) data acquired at scan rates ranging from 50 mV/s to 15 V/s.

$$\log k = \alpha \log(1-\alpha) + (1-\alpha)\log\alpha - \log(RT/nFv) - \alpha(1-\alpha)nF\Delta E_p / 2.3RT \quad (2)$$

Where k is the rate constant of the electron transfer (s^{-1}), n is the number of electrons per molecule for reduction, F is the Faraday constant (C/equiv), T is the thermodynamic temperature (K), R is the gas constant (J/(mol*K)).

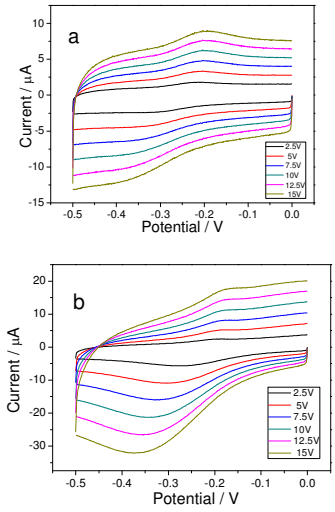

Figure 4: Cyclic voltammetry of dsDNA with (T-T)$_1$ (a) and (T-Hg(II)-T)$_1$ (b) in 10mM PBS (pH 7.4)with different scan rates.

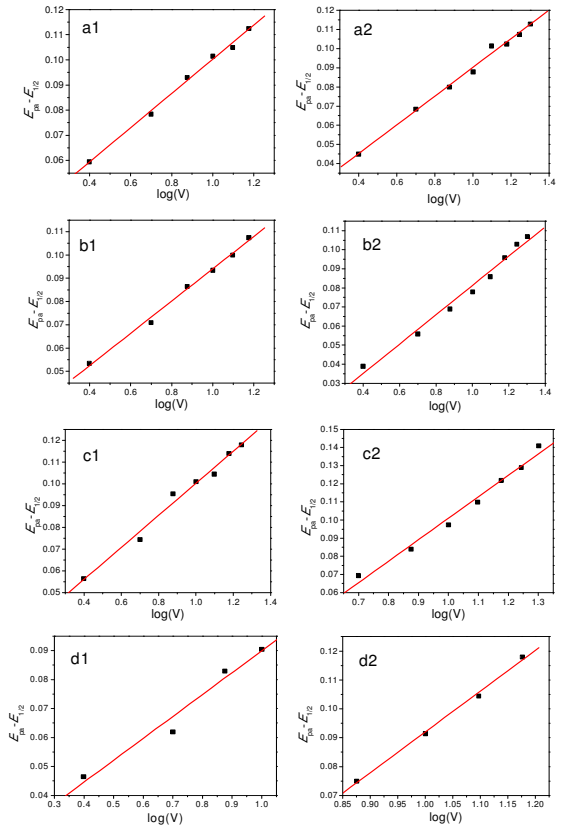

Figure 5: The fitting line of E_{pa}-$E_{1/2}$ vs log(v) with different sample: matched dsDNA (a1) and treated with Hg(II) ions(a2), dsDNA with $(TT)_1$(b1) and (T-Hg(II)-T)$_1$ (b2), dsDNA with $(TT)_3$ (c1) and (T-Hg(II)-T)$_3$(c2), dsDNA with $(TT)_6$ (d1) and with (T-Hg(II)-T)$_6$ (d2).

Table 1: The charge transfer rates (k/s^{-1}) of dsDNA with different $(TT)_n$ or (T-(Hg)-T)$_n$.

	$(TT)_0$	(T-(Hg)-T)$_0$	$(TT)_1$	(T-(Hg)-T)$_1$	$(TT)_3$	(T-(Hg)-T)$_3$	$(TT)_6$	(T-(Hg)-T)$_6$
k/s^{-1}	17.63	29.75	20.03	37.13	21.57	34.54	32.89	37.58

DNA molecules containing no TT mismatches, addition of Hg^{2+} ions increased CT kinetics. Matched DNA molecules containg AT base pairs, which will form A-Hg-T complex.[21] TT mismatches increased CT kinetics and T-Hg-T complex increased the kinetic further (Table 1). But DNA molecules containing $(TT)_{12}$ and (T-Hg(II)-T)$_{12}$ was not suitable for DNA duplex mediated electrochemical CT study (Scheme 1).

Obviously, $(TT)_n$ mismatch or (T-Hg(II)-T)$_n$ complex increased CT kinetics. DNA base pair mediated CT process is conformation-dependent. And the redox probe molecules also are capable of being reduced directly by the surface of the electrode (direct CT process).[27,28] The extent to which this mechanism contributes to the observed signal was found to be directly influenced by assembly conditions or conformation of SAM or depended on the DNA packing density. In this work, form AFM, DNA molecules containing $(TT)_{n\leq6}$, form compact DNA SAM. So the CT kinetics may be regarded as the base pair or T-Hg-T complex mediated process, but not direct elctrochemical process of the attached redox probe molecules. From AFM, the DNA SAM containing $(TT)_n$ or (T-Hg(II)-T)$_n$ bend and the height decreased slightly, so the direct CT process may contribute to the faster CT kinetics. However, this can be avoided because high scan rates were used in CV study, and it has been reported that increasing scan rates can minimize the contributions from the direct CT process.[29] The $(TT)_n$ might have π-overlapping than matched base pairs and the intercalation of Hg(II) into TT may further increase this overlapping. It has been reported that ionic complex adsorbed onto DNA backbone facilitate CT process,[28] Hg(II) ions form T-Hg-T complex, and it will not adsorbed at the backbone and CT mechanism may originate from the mediation of π-overlapting of T-Hg-T complex.

In summary, dsDNA monolayer with different (TT)n mismatched sequence were assembled onto Au(111) facet or Au electrode. The conformation or morphology, kinetics of CT process showed a $(TT)_n$ sequence-dependence. When n $\leqslant$ 6, dsDNA with $(TT)_n$ can hybridize well to form duplexes structure. The (TT)n might have π-overlapping than matched base pairs and the intercalation of Hg(II) into TT may further increase this overlapting, causing a faster CT kinetics. When n $\geqslant$ 12, dsDNA with $(TT)_{12}$ sequence can not be able to hybridize to form duplexes. And in presence of Hg(II), DNA strands hybridize via (T-Hg(II)-T)$_n$ between different DNA molecules and in this case dsDNA with $(TT)_{12}$ was not suitable for study of CT process via π-stacking within the dsDNA.

Acknowledgement

J. L. thanks Natural Science Foundation of China for Funding (20110706) and Open Project Program of Shandong Provincial Key Lab of Test Technology on Food Quality and Safety.

Notes and references

1 Genereux, J. C.; Barton, J. K. *Chem. Rev.* 2010, **110,** 1642.
2 Delaney, S.; Barton, J. K. *J. Org. Chem.* 2003, **68**, 6475.
3 Genereux, J. C.; Boal, A. K.; Barton, J. K. *J. Am. Chem. Soc.* 2010, **132,** 891.
4 Kelley, S. O.; Barton, J. K.; Jackson, N. M.; Hill, M. G. *Bioconjugate Chem.* 1997, **8**, 31.
5 Kelley, S. O.; Jackson, N. M.; Hill, M. G.; Barton, J. K. *Angew. Chem., Int. Ed.* 1999, **38**, 941.
6 Boon, E. M.; Jackson, N. M.; Wightman, M. D.; Kelley, S. O.; Hill, M. G.; Barton, J. K. *J. Phys. Chem. B* 2003, **107**, 11805.
7 Murphy, C. J.; Arkin, M. R.; Jenkins, Y.; Ghatlia, N. D.; Bossmann, S. H.; Turro, N. J.; Barton, J. K. *Science* 1993, **262**, 1025.
8 Murphy, C. J.; Arkin, M. R.; Ghatlia, N. D.; Bossman, S. H.; Turro, N. J.; Barton, J. K. *Proc. Natl. Acad. Sci. U.S.A.* 1994, **91**, 5315.
9 Hall, D. B.; Holmlin, R. E.; Barton, J. K. *Nature* 1996, **382**, 731.
10 Kawai, K.; Kodera, H.; Majima, T. *J. Am. Chem. Soc.* 2010, **132**, 14216.
11 Boon, E. M.; Barton, J. K. *Bioconjugate Chem.* 2003, **14**, 1140.
12 Kelley, S. O.; Boon, E. M.; Barton, J. K.; Jackson, N. M.; Hill, M. G. *Nucl. Acids Res.* 1999, **27**, 4830.
13 Boal, A. K.; Barton, J. K. *Bioconjugate Chem.* 2005, **16**, 312.

14 Boon, E. M.; Salas, J. E.; Barton, J. K. *Nat. Biotechnol.* 2002, **20**, 282.
15 Wong, E. L. S.; Gooding, J. J. *J. Am. Chem. Soc.* 2007, **129**, 8950.
16 Boussicault, F.; Robert, M. *Chem. Rev.* 2008, **108**, 2622.
17 Halliwell, B.; Aruoma, O. I. *FEBS Lett.* 1991, **281**, 9.
18 Imlay, J. A.; Linn, S. *Science* 1988, **240**, 1302.
19 Cooke, M. S.; Evans, M. D.; Dizdaroglu, M.; Lunec, J. *FASEB J.* 2003, **17**, 1195.
20 Guo, Q.; Yue, Q.; Zhao, J.; Wang, L.; Wang, H.; Wei, X.; Liu, J.; Jia, J. *Chem. Commun.* 2011, **47**, 11906.
21 Takezawa, Y.; Shionoya, M. *Acc. Chem. Res.* 2012, **45**, 2066.
22 Katz, S. *Biochim. Biophys. Acta* 1963, **68**, 240.
23 Miyake, Y.; Togashi, H.; Tashiro, M.; Yamaguchi, H.; Oda, S.; Kudo, M.; Tanaka, Y.; Kondo, Y.; Sawa, R.; Fujimoto, T.; Machinami, T.; Ono, A. *J. Am. Chem. Soc.* 2006, **128**, 2172.
24 Liu, S.; Clever, G. H.; Takezawa, Y.; Kaneko, M.; Tanaka, K.; Guo, X.; Shionoya, M. *Angew. Chem., Int. Ed.* 2011, **50**, 8886.
25 Kratochvílová, I.; Golan, M.; Vala, M.; Špérová, M.; Weiter, M.; Páv, O.; Šebera, J.; Rosenberg, I.; Sychrovský, V.; Tanaka, Y.; Bickelhaupt, F. M. *J. Phys. Chem. B* 2014, **118**, 5374.
26 Steel, A. B.; Herne, T. M.; Tarlov, M. J. *Anal. Chem.* 1998, **70**, 4670.
27 Pheeney, C. G.; Barton, J. K. *Langmuir* 2012, **28**, 7063.
28 Abi, A.; Ferapontova, E. E. *J. Am. Chem. Soc.* 2012, **134**, 14499.
29 Yang, W.; Lai, R. Y. *Langmuir* 2011, **27**, 14669.
30 Slinker, J. D.; Muren, N. B.; Renfrew, S. E.; Barton, J. K. *Nat. Chem.* 2011, **3**, 228.